



Research paper

## New Azepino[4,3-*b*]indole derivatives as nanomolar selective inhibitors of human butyrylcholinesterase showing protective effects against NMDA-induced neurotoxicity

Modesto de Candia, Giorgia Zaetta, Nunzio Denora, Domenico Tricarico, Maria Majellaro, Saverio Cellamare, Cosimo D. Altomare\*

Department of Pharmacy – Drug Sciences, University of Bari “A. Moro”, Via E. Orabona 4, 70125 Bari, Italy

## ARTICLE INFO

## Article history:

Received 3 July 2016

Received in revised form 9 September 2016

Accepted 12 September 2016

Available online xxx

## Keywords:

Alzheimer's disease

Azepino[4,3-*b*]indole

Butyrylcholinesterase

*N*-Methyl D-aspartate receptor

Neuroprotection

## ABSTRACT

Several 6-substituted 3,4,5,6-tetrahydroazepino[4,3-*b*]indol-1(2*H*)-one (THAI) derivatives were synthesized and evaluated for their activity as cholinesterase (ChE) inhibitors. The most potent inhibitors were identified among 6-(2-phenylethyl)-THAI derivatives, and in particular compounds **12b** and **12d** proved to be very active against human BChE (IC<sub>50</sub> = 13 and 1.8 nM, respectively), with 1000-fold selectivity over AChE. Structure-activity relationships highlighted critical features (e.g., ring fusion [4,3-*b*], integrity of the lactam CONH function) and favorable physicochemical properties of the 6-(2-phenylethyl) group (i.e., optimal position, size and lipophilicity of phenyl substituents). The effects of a number of compounds against NMDA-induced SH-SY5Y neuronal cell injury were also evaluated. Treatment with **12b** increased cell viability in SH-SY5Y cells pretreated with 250 μM NMDA, with significant effects (*P* < 0.05) at concentrations between 0.5 and 5 μM. These findings suggest that THAI can be used as a scaffold for developing new drug leads for the treatment of Alzheimer-type neurodegeneration syndrome.

© 2016 Published by Elsevier Ltd.

## Abbreviations

AD	Alzheimer Disease
ACh	Acetylcholine
AChE	Acetylcholinesterase
BChE	Butyrylcholinesterase
CAS	Catalytic anionic site
CNS	Central Nervous System
DCM	dichloromethane
DMEM	Dulbecco's modified eagle's medium
DMSO	Dimethyl sulfoxide
FBS	Fetal bovine serum
5-FU	5-fluorouracil
HB	Hydrogen bond
HepG2	human hepatocellular carcinoma cell line
LAH	Lithium Aluminum Hydride
MTT	3-(4,5-dimethylthiazol-2-yl)-2,5-diphenyltetrazolium bromide
MCF-7	human breast carcinoma cell line
NMDA	<i>N</i> -methyl- <i>D</i> -aspartate
NMDAR	<i>N</i> -methyl- <i>D</i> -aspartate receptor
PAS	Peripheral anionic site
PB	Phosphate Buffer

PBS	Phosphate Buffered Saline
SAR	Structure-activity relationship
SH-SY5Y	human neuroblastoma cell line
TBAB	Tetrabutyl ammonium bromide
TFA	Trifluoro acetic acid
U-87	human glioblastoma cell line

## 1. Introduction

Neurodegeneration in Alzheimer's disease (AD), a devastating disorder accounting for the majority of the dementias, is primarily characterized by histopathological hallmarks, namely the presence of intracellular neurofibrillary tangles of hyperphosphorylated  $\tau$ -protein and extracellular  $\beta$ -amyloid protein deposits contributing to senile plaques, and lower levels of the neurotransmitter acetylcholine (ACh) [1]. Despite the advances achieved over the last two decades in understanding the pathogenic mechanisms underlying AD, only a few drugs have been approved. The currently available treatments (Chart 1) include acetylcholinesterase (AChE, EC 3.1.1.7) inhibitors **1–3** (rivastigmine, galantamine, and donepezil), approved for the symptomatic relief of mild to moderate AD, and the *N*-methyl-*D*-aspartate receptor (NMDAR) antagonist **4** (memantine) [2].

Galantamine and donepezil are reversible cholinesterase (ChE) inhibitors, whereas rivastigmine is a pseudo-irreversible inhibitor which transfers a carbamate moiety to the Ser residue (followed by slow hydrolysis) in the active sites of AChE and butyryl-

\* Corresponding author.

Email address: cosimodamiano.altomare@uniba.it (C.D. Altomare)

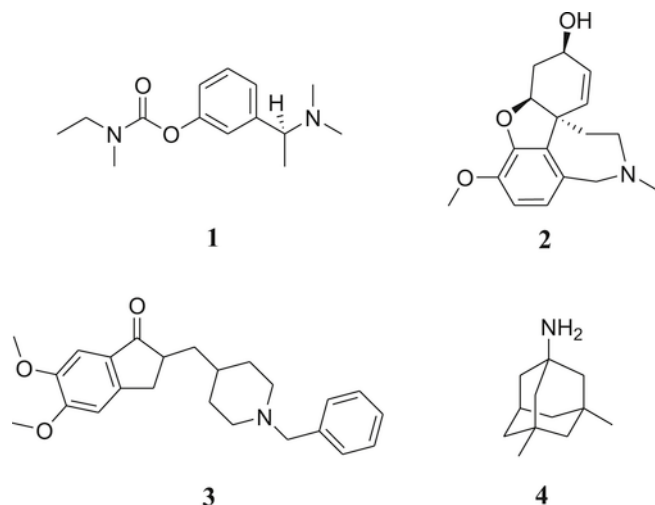


**Chart 1.** Currently available drugs for the therapeutic management of AD. Rivastigmine (1), galantamine (2) and donepezil (3) are ChE inhibitors; memantine (4) is NMDAR antagonist.

cholinesterase (BChE, EC 3.1.1.8). The impairment of ACh neurotransmission is a downstream process in the cognitive deficit accompanying AD; therefore a role of ChE inhibitors leading to a recovery of the cholinergic neurotransmission and related beneficial effects on cognition capacity has long been postulated [3]. AD patients may further benefit from reduction of glutamate-induced,  $\text{Ca}^{2+}$ -mediated excitotoxicity by the NMDAR antagonist memantine (4). Based on the available data, it may be supposed that new small molecules which simultaneously target both cholinergic transmission and glutamate-induced excitotoxicity may improve the AD pharmacological treatment [4,5].

ACh is mainly hydrolyzed by AChE in the synaptic cleft of the cholinergic neurons, but at higher concentrations is also hydrolyzed by BChE, which is produced in liver and found primarily in plasma where it is also responsible for detoxification of xenobiotics [6,7]. BChE is also localized in CNS glial cells and neurons, where it works as a co-regulator of cholinergic neurotransmission [8]. It has been found that BChE can compensate AChE catalytic functions in synaptic cleft and its activity increases by 30–60% during the time course in AD [9–12].

Selective BChE inhibitors usually contain tri- or polycyclic structures (Chart 2). For instance, physostigmine has been taken as a scaffold to synthesize selective irreversible BChE inhibitors, such as *N*<sup>1</sup>-phenetylnorcymserine (irreversible) [8,13], whereas phenothiazine derivatives (e.g., ethopropazine) [14] and some quinazolinimine-based compounds proved to be selective reversible BChE inhibitors [15].

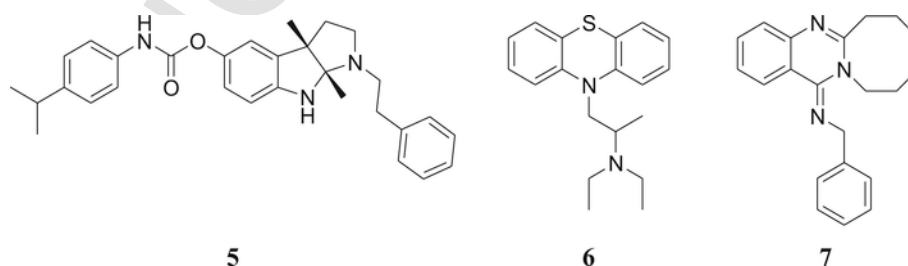


**Chart 2.** Structures of recently reported BChE inhibitors: *N*<sup>1</sup>-phenetylnorcymserine (5), ethopropazine (6); quinazolinimine derivative (7).

AChE and BChE, which share about 70% of homology and retain the same key residues in the choline binding pocket, differ for their three-dimensional (3D) structures. AChE contains a 20 Å deep and narrow gorge, in which five regions are involved in the ligand binding: (i) the catalytic triad residues (Ser203, His447, Glu334); (ii) the ‘oxyanion hole’ inside the active center, that stabilizes the transient tetrahedral enzyme-substrate complex by accommodation of negatively charged carbonyl oxygen; (iii) the ‘anionic site’ (AS), where Trp86 (a residue conserved in all ChEs), involved in the orientation and stabilization of trimethylammonium group of ACh, through cation- $\pi$  interactions; (iv) the ‘acyl pocket’ interacting with the substrate acyl group; (v) the ‘peripheral anionic site’ (PAS), located on the rim of the active site gorge [16]. The main differences between AChE and BChE occur in the ‘acyl pocket’ and PAS. Two Phe residues (Phe295, Phe297) in the ‘acyl pocket’, which prevent the access of bulkier molecules to the catalytic site in AChE, are replaced by two aliphatic residues (Leu286, Val288) in BChE, whereas globally six of the fourteen AChE aromatic residues encompassing the ‘acyl pocket’ and PAS in AChE are replaced by aliphatic residues in BChE. This ultimately results in *ca.* 200 Å<sup>3</sup> larger gorge in BChE than in AChE [17–20].

In previous work, we reported the ChEs' inhibitory activity of a number of diverse ester derivatives of annulated tetrahydroazocines, showing that some compounds containing two isomeric 2,3,6,11-tetrahydro-1*H*-azocino[4,5-*b*]indole and 2,3,6,7-tetrahydro-1*H*-azocino[5,4-*b*]indole scaffolds preferentially inhibited AChE over BChE, with potency in the low micromolar range [21,22]. In this study, in order to obtain more information on ChEs' inhibition activity and selectivity of indole-containing tricycle derivatives, we focus on a series of compounds bearing partially hydrogenated azepino[4,3-*b*]indole as core structure. In particular, 3,4,5,6-tetrahydroazepino[4,3-*b*]indol-1(6*H*)-one (THAI) [22] was taken as scaffold, and a number of diverse substituents on indole nitrogen ( $\text{N}^6$ ) and chemical modifications of the annulated heterocyclic core were investigated.

The THAI scaffold investigated herein is structurally similar to the heterocyclic core of the known drug dimebon (latrepirdine), that is a 2,3,4,5-tetrahydro-1*H*-pyrido[4,3-*b*]indole derivative showing multimodal activity with rather controversial results in clinical studies of AD patients [23]. Developed as antihistamine drug, dimebon exhibited *in vitro* activities against ion channels (e.g., L-type calcium channels), receptors and neurotransmitter systems (e.g., AMPA, NMDA, glutamate,  $\alpha$ -adrenergic and serotonergic 5-HT<sub>2C</sub>, 5-HT<sub>5A</sub>, 5-HT<sub>6</sub> receptors), and ChEs inhibition (preference for BChE) with potencies in the micromolar range [24–27].

Taking in mind the neuroprotective effects of the NMDAR antagonists (e.g., memantine 4) and the structural resemblance between the THAI scaffold and the heterocyclic core of dimebon, which also showed NMDAR antagonist properties, a number of synthesized compounds, exhibiting elevated BChE inhibition potency, were also

assayed for their activity in an NMDA-induced neuronal cells death model.

## 2. Chemistry

Most of the 6-substituted derivatives of 3,4,5,6-tetrahydroazepino[4,3-*b*]indol-1(*2H*)-one (**10a**) and 3,4,5,6-tetrahydroazepino[3,2-*b*]indol-2(*1H*)-one (**16**) were synthesized as shown in Scheme 1.

As previously reported by others [28], phenylhydrazine or (4-fluorophenyl)hydrazine were reacted with 1,3-cyclohexanedione to provide the respective hydrazones which, by treatment with refluxing trifluoroacetic acid (TFA) under Fisher conditions, afforded the 1,2,3,9-tetrahydro-4*H*-carbazol-4-one derivatives **8a** and **8b** (65–70% yields). Compounds **8a,b** were converted into the corresponding ketoximes **9a,b**, which then underwent a selective Beckmann rearrangement by treatment with preheated PPA at 110 °C to provide the [4,3-*b*] THAI products **10a** (unsubstituted) and **10b** (9-*F* substituted) in high yield (>70%), as shown by a triplet signal ( $\delta$  7.43 ppm) of the lactam NH in the <sup>1</sup>HNMR spectrum; under these reaction conditions negligible amounts of the [3,2-*b*] ring fusion isomers were found.

Regioselective alkylation by suitable alkyl halides was achieved at the indole nitrogen (N<sup>6</sup>), and not at the lactam nitrogen (N<sup>1</sup>) of **10a** and **10b**, as shown by the <sup>1</sup>HNMR disappearance of N<sup>6</sup>—H proton singlet ( $\delta$  11.40 ppm), in the presence of TBAB as the phase transfer catalyst in stirred DCM/25% NaOH biphasic mixtures (24–72 h at rt or 40 °C), affording **11a–d** and **12a–h** (X = H), and **12i** (X = F). Then, nitrile reduction of **11d** by CoCl<sub>2</sub> and NaBH<sub>4</sub> gave the 6-(2-aminoethyl)-THAI derivative **11e**, which was then reacted with ethyl chloroformate to afford the ethylcarbamate **11f**. Methylation reaction of 6-(2-phenylethyl)-THAI **12b** with methyl iodide in the presence of NaH yielded **13**, whereas reduction of the lactam group by lithium

aluminum hydride (LAH) gave the basic compound **14**, isolated as hydrochloride salt.

The THAI derivative **17**, that is the [3,2-*b*] ring fusion isomer of **12b**, was synthesized starting from **9a**, which was first treated with tosyl chloride, and the produced sulphonyl oxime **15** refluxed in a toluene suspension with aluminum oxide to afford **16** [29], that was finally alkylated by 2-phenethyl bromide under the above conditions.

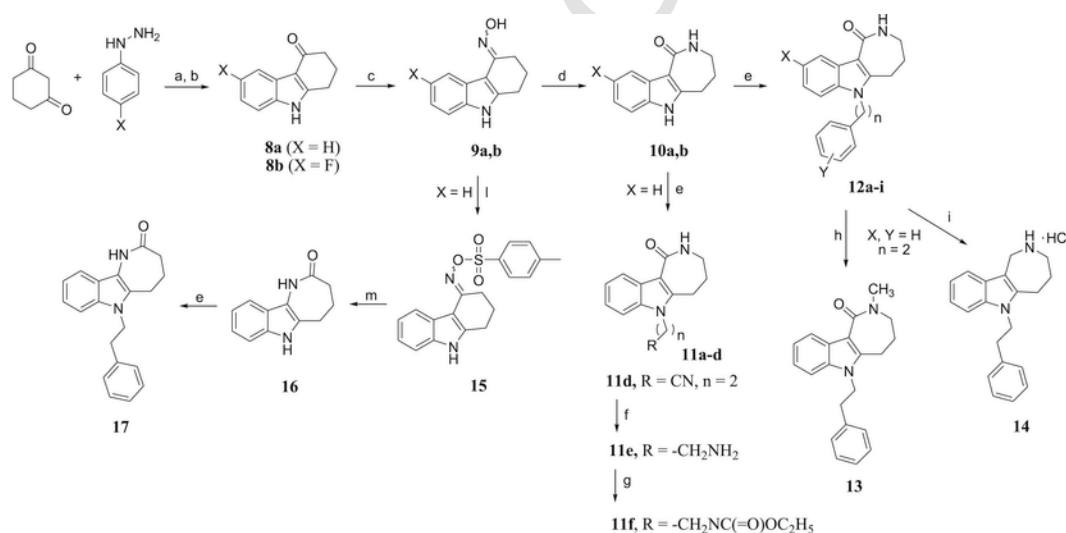
The synthesis of the ketoxime derivative **19** was accomplished as shown in Scheme 2.

Compound **22**, designed as ring-opened analogue of **12b**, was also synthesized (Scheme 3). The commercially available methyl 1*H*-indole-3-carboxylate was first alkylated by reaction with phenethyl bromide to afford **20**, which underwent subsequent ester hydrolysis (**21**) and coupling with *n*-propylamine to provide the amide derivative **22**.

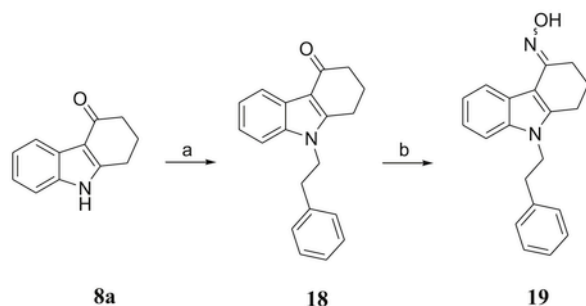
## 3. Results and discussion

The 6-substituted THAI-based synthesized compounds were tested for their inhibitory activity toward electric eel AChE and horse serum BChE, using the Ellmann colorimetric assay (galantamine as the reference standard) [22,30]. The half maximal inhibitory concentration (IC<sub>50</sub>) values or the inhibition percentages at 10 μM concentration are reported in Tables 1 and 2.

The THAI derivatives bearing diverse moieties on the indole nitrogen (Table 1) selectively inhibited BChE. The 6-(2-phenylethyl) group (**12b**) proved to inhibit BChE in the nanomolar range (IC<sub>50</sub> = 24 nM) with 830-fold selectivity over AChE. Compound **12b** proved to be not only much more potent than the lower (**12a**) and higher (**12c**) homologues, bearing 6-benzyl and 6-(3-phenylpropyl) groups, respectively, but also more potent than other 6-substituted derivatives bearing isopropyl (**11a**), ester (**11b,c**) and carbamate (**11f**) groups. A fluorine atom in the *meta*-position (and not in *para*) of

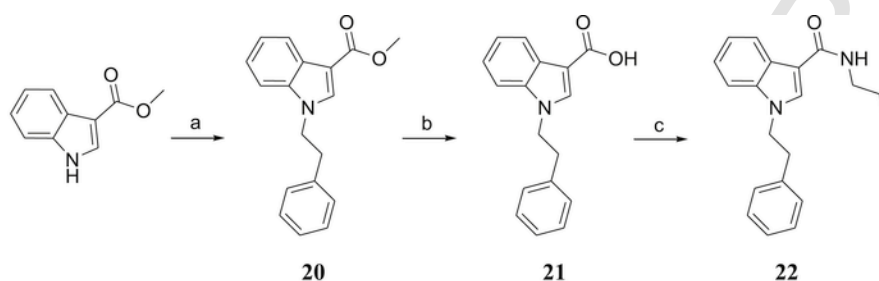


**Scheme 1.** Synthesis of 6-substituted 3,4,5,6-tetrahydroazepino[4,3-*b*]indol-1(*2H*)-one (**11–14**) and 3,4,5,6-tetrahydroazepino[3,2-*b*]indol-2(*1H*)-one (**17**) derivatives<sup>a</sup>. <sup>a</sup> Reagents and conditions: a) Water, rt, overnight, 85%; b) TFA, reflux, 24 h, 65–70%; c) NH<sub>2</sub>OH × HCl, AcONa, EtOH/H<sub>2</sub>O 2/1 v/v, reflux, 24 h, 85–90%; d) 110 °C-preheated PPA, 30 min, 70%; e) appropriate alkyl halide, TBAB, 25% NaOH/DCM 1/3 v/v, rt or 40 °C, 48 h, 35–75%; f) CoCl<sub>2</sub> × 6H<sub>2</sub>O, NaBH<sub>4</sub>, MeOH, 0 °C to rt, 2 h, 76%; g) **11e**, ethyl chloroformate, TEA, dry THF, rt, overnight, 60%; h) NaH, CH<sub>3</sub>I, dry DMF, rt, 24 h, 40%; i) (1) LAH, dry dioxane, reflux, 18 h, 50%; (2) 1.25 M HCl/MeOH, rt, 50%; l) tosyl chloride, DMAP, dry DCM, 4 h, 60%; m) Al<sub>2</sub>O<sub>3</sub>, toluene, rt, overnight, 53%.



<sup>a</sup> Reagents and conditions: a) Phenethyl bromide, TBAB, 25% NaOH/DCM 1/3 v/v, rt, 48 h, 60%; b) NH<sub>2</sub>OH·HCl, AcONa, EtOH/H<sub>2</sub>O 2/1 v/v, reflux, 24h, 60%.

**Scheme 2.** Synthesis of the oxime derivative of 9-(2-phenylethyl)-1,2,3,9-tetrahydro-4H-carbazol-4-one (**19**)<sup>a</sup>. <sup>a</sup> Reagents and conditions: a) Phenethyl bromide, TBAB, 25% NaOH/DCM 1/3 v/v, rt, 48 h, 60%; b) NH<sub>2</sub>OH × HCl, AcONa, EtOH/H<sub>2</sub>O 2/1 v/v, reflux, 24 h, 60%.



<sup>a</sup> Reagents and conditions: a) NaH, phenethyl bromide, dry DMF, rt, 24h, 47%. b) 2N NaOH, THF, reflux, overnight, 95%. c) HOBt, DCC, *n*-propylamine, dry CH<sub>2</sub>Cl<sub>2</sub>, rt, overnight, 42%.

**Scheme 3.** Synthesis of 1-(2-phenylethyl)-*N*-propyl-1H-indole-3-carboxamide (**22**)<sup>a</sup>. <sup>a</sup> Reagents and conditions: a) NaH, phenethyl bromide, dry DMF, rt, 24 h, 47%. b) 2 N NaOH, THF, reflux, overnight, 95%. c) HOBt, DCC, *n*-propylamine, dry CH<sub>2</sub>Cl<sub>2</sub>, rt, overnight, 42%.

**Table 1**

Half maximal inhibitory concentration (IC<sub>50</sub>) values (or % inhibition values at 10 μM)<sup>a</sup> of electric eel AChE and equine BChE by 6-substituted 3,4,5,6-tetrahydroazepino[4,3-*b*]indol-1(2*H*)-one derivatives.<sup>b</sup>

Cmpd	n	R/Y-Ph	IC <sub>50</sub> (μM)	
			AChE	BChE
<b>11a</b>	2	CH(CH <sub>3</sub> ) <sub>2</sub>	100 ± 5	22.3 ± 1.3
<b>11b</b>	4	OCOCH <sub>3</sub>	(5 ± 2%)	10.7 ± 1.1
<b>11c</b>	3	COOC <sub>2</sub> H <sub>5</sub>	60.0 ± 3.5	25.7 ± 1.2
<b>11f</b>	3	NHCOOC <sub>2</sub> H <sub>5</sub>	110 ± 15	15.0 ± 1.1
<b>12a</b>	1	C <sub>6</sub> H <sub>5</sub>	(10 ± 5%)	(25 ± 10%)
<b>12b</b>	2	C <sub>6</sub> H <sub>5</sub>	20.0 ± 2.0	0.024 ± 0.004
<b>12c</b>	3	C <sub>6</sub> H <sub>5</sub>	(18 ± 5%)	(20 ± 8%)
<b>12d</b>	2	3'-F-C <sub>6</sub> H <sub>4</sub>	(5 ± 2%)	0.0015 ± 0.001
<b>12e</b>	2	4'-F-C <sub>6</sub> H <sub>4</sub>	(10 ± 7%)	0.230 ± 0.035
<b>12f</b>	2	3'-Cl-C <sub>6</sub> H <sub>4</sub>	(11 ± 8%)	0.065 ± 0.011
<b>12g</b>	2	4'-Cl-C <sub>6</sub> H <sub>4</sub>	(2 ± 2%)	1.90 ± 0.33
<b>12h</b>	2	4'-CH <sub>3</sub> -C <sub>6</sub> H <sub>4</sub>	(10 ± 5%)	68.2 ± 5.0
<b>2, galantamine</b>			0.560 ± 0.100	11.9 ± 0.3

<sup>a</sup> Seven different concentrations of each compound were used to determine IC<sub>50</sub> values by regression of the sigmoid dose-response curves through GraphPad Prism software (vers. 5.01); data are means ± SEM of at least three independent measurements.

<sup>b</sup> General structures in Scheme 1.

phenyl (**12d**) led to a 16-fold additional improvement over **12b** in BChE binding affinity on IC<sub>50</sub> scale (1.5 nM), which is translated into about 7 kJ mol<sup>-1</sup> free energy change, and remarkable decrease in

AChE inhibitory activity. With Cl in place of F no activity improvement was observed, but a similar position-related trend appeared (**12f**, *m*-Cl > **12g**, *p*-Cl).

The introduction of a *p*-Me group (**12h**) led to a sharp decrease in BChE inhibition.

Lineweaver-Burk plots outlined for the most active compound **12d** (Fig. 1), using fixed amounts of BChE and varying concentrations of the substrates between 25 and 250 μM, in the absence or presence of inhibitor at different concentrations (0.5–5 nM), clearly showed a competitive type inhibition. A replot of the slopes versus the corresponding inhibitor concentrations provided a *K<sub>i</sub>* value equal to 0.7 nM.

Some further modifications around the 3,4,5,6-tetrahydroazepino[4,3-*b*]indol-1(2*H*)-one (THAI) tricyclic scaffold were explored, choosing the 6-(2-phenylethyl) group as the constant feature (Table 2).

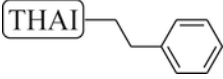
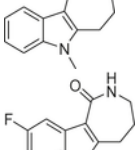
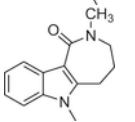
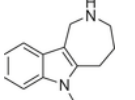
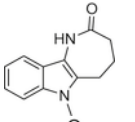
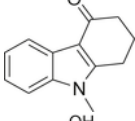
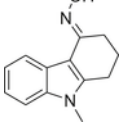
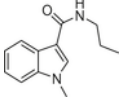
The 9-F THAI analog **12i** resulted almost equipotent with the unsubstituted parent compound **12b**. The *N*-methylation of the lactam (**13**) led to a >400-fold decrease of BChE binding affinity (>15 kJ mol<sup>-1</sup> free energy increase) and a selectivity reversal, whereas the reduction of the lactam —CONH— to —CH<sub>2</sub>NH— amine derivative **14** caused about 50-fold loss of BChE inhibition potency.

The comparison between the activities of the ring fusion isomers **12b** and **17** is noteworthy. As a matter of fact, the reversal of the directionality of —CONH— (**12b**) into —NHCO— (**17**), due to the different ring fusion between azepan-2-one and indole rings, re-



**Table 2**

Half maximal inhibitory concentration ( $IC_{50}$ ) values (or % inhibition values at  $10 \mu\text{M}$ )<sup>a</sup> of electric eel AChE and equine BChE of derivatives (**12i**, **13**, **14**), isomer (**17**) and other analogues (**18**, **19**, **22**) of 6-(2-phenylethyl)-3,4,5,6-tetrahydroazepino[4,3-*b*]indol-1(2*H*)-one (**12b**).

Cmpd	THAI	$IC_{50}$ ( $\mu\text{M}$ )	
		AChE	BChE
<b>12b</b>		$20.0 \pm 2.0$	$0.024 \pm 0.004$
<b>12i</b>		$(5 \pm 2\%)$	$0.028 \pm 0.002$
<b>13</b>		$44.8 \pm 2.5$	$(10 \pm 7\%)$
<b>14</b>		$(33 \pm 10\%)$	$1.14 \pm 0.03$
<b>17</b>		$(13 \pm 7\%)$	$(25 \pm 8\%)$
<b>18</b>		$10.0 \pm 1.5$	$10.0 \pm 0.3$
<b>19</b>		$(16 \pm 10\%)$	$(5 \pm 5\%)$
<b>22</b>		$10.3 \pm 1.7$	$12.6 \pm 3.1$

<sup>a</sup> See footnote of Table 1.

sulted in a marked drop of BChE (and AChE as well) binding affinity.

The enzyme inhibition data of **17**, compared with those of **12b**, pointed out that the lactam  $\text{CONH}$  group of THAI core should be involved in directional HB interactions within the BChE binding site. In addition, spectrophotometric evidence led us to exclude that the fusion isomer lactam derivatives **12b** and **17** may undergo any (different) inactivating BChE-catalyzed amide hydrolysis [31], remaining both stable when incubated with the enzyme for 1 h (see Supplementary material). We could therefore reasonably hypothesize that HB interactions with the BChE binding pocket should be more efficiently achieved with the [4,3-*b*] ring fusion in **12b** and other analogs, which become critical to well allocate the 6-(2-phenylethyl)-THAI inhibitors into the BChE binding site [32]. At the best of our knowledge, the role of such a kind of HB interactions has not been pointed out for other tricyclic BChE-selective reversible inhibitors.

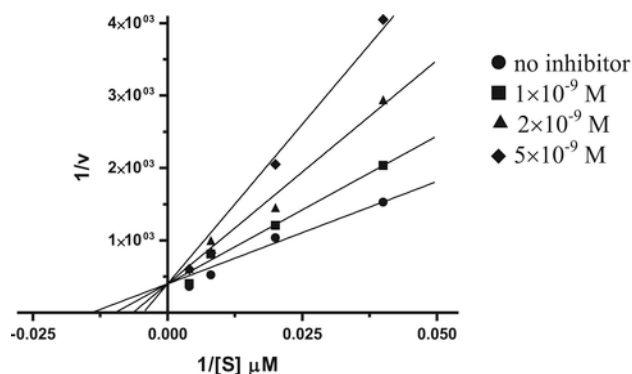


**Fig. 1.** Inhibition kinetics of **12d** using Lineweaver–Burk plots ( $r^2 \geq 0.984$ ) with equine BChE ( $0.09 \text{ U/mL}$ ) and different substrate (butyrylthiocholine iodide) concentrations ( $25\text{--}250 \mu\text{M}$ ); replot ( $r^2 \geq 0.986$ ) of the slopes versus  $[I]$  to determine  $K_i$  ( $0.7 \text{ nM}$ ) as the *x*-axis intercept is shown in the upper left insert.

Finally, the decrease of BChE inhibition potency shown by the 4*H*-carbazol-4-one derivatives **18** and **19** is somehow in line with expectations, taking in mind that BChE active site, compared with that of AChE, should better accommodate larger scaffolds. The *N*-propylcarboxamide **22** as the ring opening analog of **12b**, likely due to entropic factors, proved to be about 500-fold less potent BChE inhibitor, while increasing inhibition activity toward AChE. The main SARs of 6-substituted THAI-based inhibitors are summarized in Fig. 2.

The THAI derivatives **12b**, **12d** and **12e** were also tested as inhibitors of human ChEs, which are known to share high (>80%) structural homology with electric eel AChE and horse serum BChE (Table 3). Interestingly, compounds **12b** and **12d** did not exhibit any noteworthy species-dependent ChEs' inhibition activity and selectivity, whereas the 4'*F*-phenethyl THAI derivative **12e** proved less potent and selective in human ChEs.

Finally, four active BChE inhibitors (**12b**, **12d**, **12e** and **14**) were tested for their effects on cell viability by exposing human neuroblastoma (SH-SY5Y) cell line [33–35] to the compounds at increasing concentrations from  $0.1 \mu\text{M}$  to  $1 \text{ mM}$  during 72 h. Cell viability was assessed by (3,4,5-dimethylthiazol-2-yl)-2,5-diphenyltetrazolium

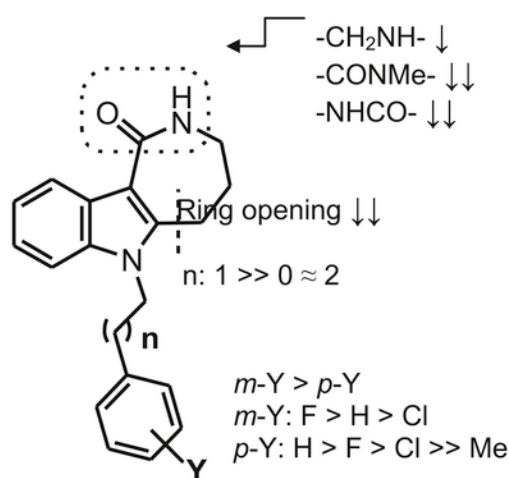


**Fig. 2.** Structure-activity relationships of 6-substituted 3,4,5,6-tetrahydroazepino[4,3-*b*]indol-1(2*H*)-one-based inhibitors of horse serum BChE around the structure of **12b**. Symbols:  $\downarrow$  and  $\gg$ , less than 100-fold decrease and increase, respectively, in  $IC_{50}$ ;  $\downarrow\downarrow$  and  $\gg\gg$ , more than 100-fold decrease and increase, respectively, in  $IC_{50}$ ;  $\dagger$ , bond break.

**Table 3**

Half maximal inhibitory concentration (IC<sub>50</sub>) values (or % inhibition values at 10 μM)<sup>a</sup> of human AChE and BChE of selected 6-(*Y*-phenylethyl)-3,4,5,6-tetrahydroazepino[4,3-*b*]indol-1(2*H*)-one derivatives.

Cmpd	IC <sub>50</sub> (μM)	
	<i>h</i> AChE	<i>h</i> BChE
<b>12b</b>	12.6 ± 1.2	0.013 ± 0.005
<b>12d</b>	(6 ± 4%)	0.0018 ± 0.001
<b>12e</b>	10.0 ± 4.3	5.00 ± 1.03

<sup>a</sup> See footnote of Table 1.

bromide (MTT) assay. The NMDAR antagonist memantine (**4**) [36,37] was also tested in this assay. The test compounds affected SH-SY5Y cell viability in a dose dependent manner (plots in Supplementary material), and the respective concentration for half maximal inhibition of cell proliferation (GI<sub>50</sub>) values are reported in Table 4.

Compound **12d** and the amino derivative **14** caused a 50%-reduction of SH-SY5Y cell viability at concentrations in the low micromolar range (GI<sub>50</sub> values equal 2.61 and 5.60 μM, respectively). In contrast, **12b** (GI<sub>50</sub> = 138 μM) and **12e** (GI<sub>50</sub> = 251 μM) showed cytotoxicity on human neuroblastoma cells at doses close to or higher than **4** (GI<sub>50</sub> = 145 μM).

Compounds **12b**, **12d**, **12e** and **14** were further tested in a panel of cultured tumor cells, namely human glioblastoma (U-87), human breast carcinoma (MCF-7) and human hepatocellular carcinoma (HepG2) cell lines, using 5-fluorouracil (5-FU) as the positive control (Table 4). Compound **14** proved to be toxic enough with GI<sub>50</sub>'s in the low micromolar range (25–41 μM), whereas the lactam derivatives **12b**, **12d** and **12e** showed significant cytotoxicity in the three cell lines at doses >100 μM, their GI<sub>50</sub>'s being of the same order of magnitude as those reported for tacrine (a known AChE inhibitor) in HepG2 cells [33].

Finally, compounds **12b**, **12d**, **12e**, **14** and memantine (**4**) were assayed in vitro for their ability to counteract the NMDA-induced toxicity in SH-SY5Y cells. The neuronal cells were exposed to NMDA (250 μM, i.e. a concentration close to its GI<sub>50</sub>; see Supplementary material) in co-treatment with various concentrations of test compounds (0.1, 0.5, 1 and 5 μM), and cell viability was determined by MTT assay. As shown in Fig. 3, NMDA decreased viable cells, which resulted ca. 40% lower than the NMDA-untreated cells. Memantine (**4**) showed statistically significant protective effects against

**Table 4**

Effect of selected compounds on the cell viability of human SH-SY5Y neuroblastoma, U-87 glioblastoma, MCF-7 breast cancer and HepG2 hepatocellular carcinoma cell lines.

Cell line	GI <sub>50</sub> (μM) <sup>a</sup>					
	<b>12b</b>	<b>12d</b>	<b>12e</b>	<b>14</b>	<b>4</b>	5-FU
<b>SH-SY5Y</b>	138 ± 28	2.61 ± 1.2	251 ± 11	5.60 ± 0.5	145 ± 14	–
<b>U-87</b>	288 ± 13	162 ± 2.8	>500	41 ± 3.3	–	13 ± 0.3
<b>MCF-7</b>	170 ± 4.2	162 ± 5.7	>500	28 ± 0.9	–	4.5 ± 0.5
<b>HepG2</b>	120 ± 23	159 ± 22	230 ± 19	25 ± 1.0	–	7.0 ± 0.5

<sup>a</sup> Effect on cell viability expressed as the concentration for half maximal inhibition of cell proliferation (GI<sub>50</sub>); data are means ± SEM. Cells were seeded at a density of ~5000 cells/well. After 24 h of incubation at 37 °C in humidified atmosphere with 5% CO<sub>2</sub>, the culture medium was replaced with fresh medium containing different concentrations of the test compounds and incubated for 48 h. Cell viability was assessed by the MTT assay. Cells without test compounds were used as positive controls.

NMDA-induced injury only at 5 μM (68.0% viability, *P* < 0.01; Fig. 3e).

Treatment with **12b** increased cell viability (Fig. 3a), exhibiting significant effects at 0.5 μM and higher protection at 5 μM concentration (76.9% viable cells, *P* < 0.001). A similar trend (Fig. 3c) was shown by the 4'-phenyl THAI derivative **12e** (76.6% viable cells, *P* < 0.001, at 5 μM). In contrast, compound **12d** (3'-phenylethyl-bearing THAI derivative; Fig. 3b) and the amino derivative **14** (Fig. 3d) showed maximal protective activity at 0.5 μM (70% and 76% viable cells, respectively) with a decrease of activity at higher doses. Both compounds did not exhibit significant SH-SY5Y protection at 5 μM concentration. This trend could most likely be explained taking into account the observed intrinsic toxicity of **12d** and **14** in SH-SY5Y neuronal cells (GI<sub>50</sub> values equal 2.61 and 5.60 μM, respectively).

In summary, the above findings led us to identify **12b** as potent and selective inhibitor of human BChE (IC<sub>50</sub> = 13 nM; 1000-fold selectivity over *h*AChE), endowed with moderate protective effects in SH-SY5Y cell-based model of NMDA-induced toxicity. In this assay, **12b** proved to be even more active than memantine (**4**). Moreover, **12b** did not show in vitro remarkable hepatotoxicity, assessed as cell viability in HepG2 cell [38], whereas, compared to the stronger *h*BChE inhibitor **12d** (IC<sub>50</sub> = 1.8 nM; >>5000-fold selectivity over *h*AChE) **12b** proved to be itself much less neurotoxic, as shown by cell viability measures in SH-SY5Y cell line (GI<sub>50</sub> equals to 138 and 2.61 μM for **12b** and **12d**, respectively).

#### 4. Conclusions

A new class of selective BChE inhibitors was identified which contain the azepinoindole heterocyclic core. A number of 6-substituted 3,4,5,6-tetrahydroazepino[4,3-*b*]indol-1(2*H*)-one (THAI) derivatives achieved nanomolar IC<sub>50</sub> values against BChE and remarkable selectivity over AChE. The ring fusion isomerism appeared as a critical feature, given that [4,3-*b*] ring fusion between azepan-2-one and indole (**12b**) is required for BChE inhibitory activity, whereas [3,2-*b*] ring fusion (**17**) leads to activity loss. Besides the critical importance of the directionality of the lactam —CONH— group, SARs highlighted the following major features that allow THAI-based inhibitors to achieve efficient and selective binding into the BChE active site: (i) integrity (e.g., no lactam reduction, *N*-methylation, ring opening) of the azepan-2-one moiety, and (ii) optimal size and lipophilicity of the 6-(2-phenylethyl) group. Two 6-(2-phenylethyl)-THAI derivatives, namely **12b** and **12d**, showed competitive type inhibition, nanomolar potency against BChE and remarkable selectivity over AChE.

Toxicity investigations on liver HepG2 cells and neuronal SH-SY5Y cells, as well as a preliminary screening of neuroprotection effect against NMDA-induced toxicity in SH-SY5Y cells, led to identify **12b** as an attractive hit for further pharmacological studies on animal models of neurodegeneration and AD. Indeed, compound **12b**, which did not display any hepatotoxicity and neurotoxicity in cell models up to 10 μM, proved to be a highly potent and selective inhibitor of human BChE (IC<sub>50</sub> = 13 nM and 1000-fold selectivity over *h*AChE) showing also moderate (20–25%) protective effects against NMDA-induced neurotoxicity in an SH-SY5Y cell model at concentrations in the low micromolar range (0.5–5 μM).

In conclusion, this study provides data to support the 3,4,5,6-tetrahydroazepino[4,3-*b*]indol-1(2*H*)-one as a tricyclic scaffold for designing new potent BChE-selective inhibitors useful on one hand as molecular tools for better investigating the role of BChE in the

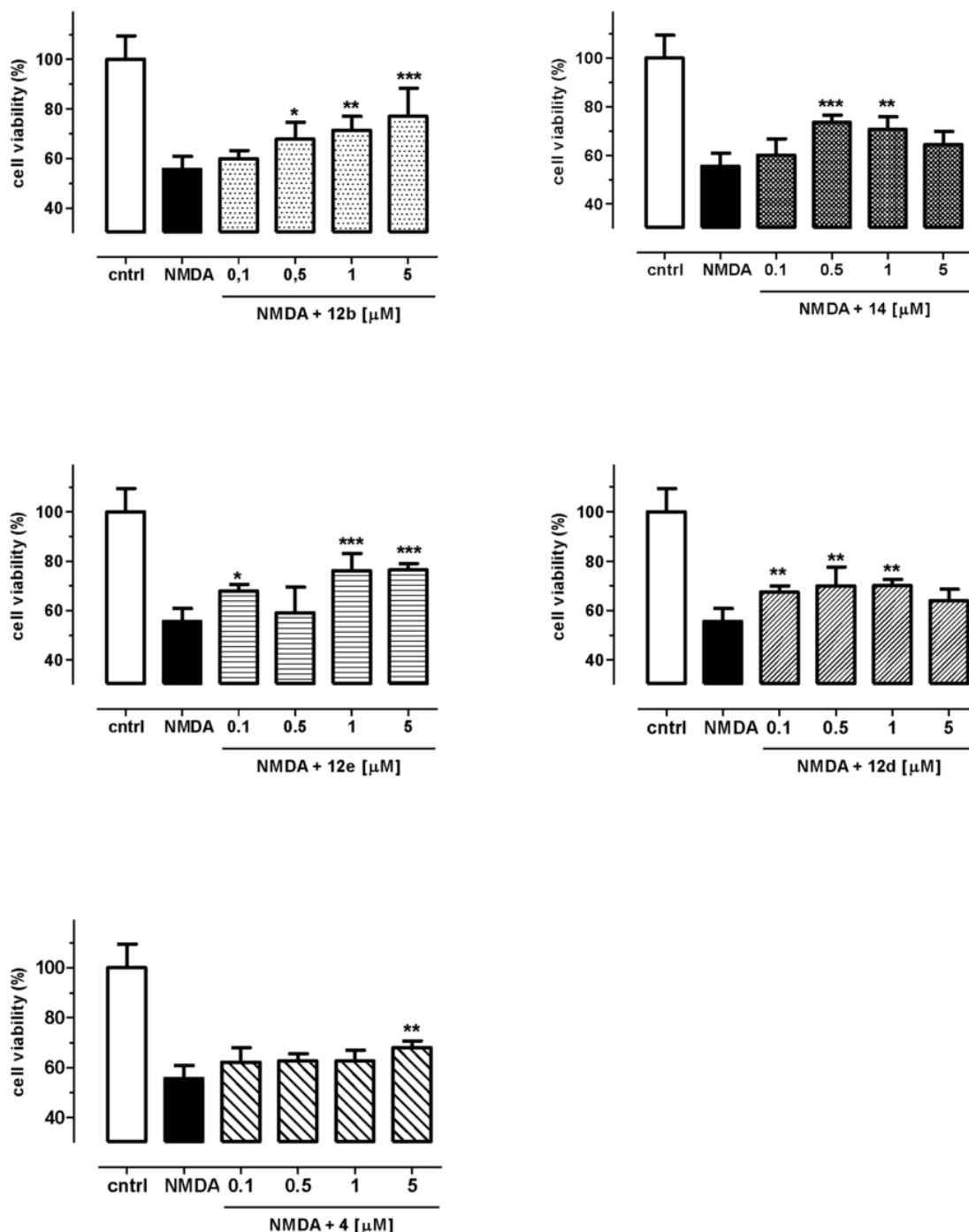


**Fig. 3.** Protective effects of compounds **12b**, **12d**, **12e**, **14** and memantine **4** at four concentrations (0.1–5 μM) on 250 μM NMDA-induced cytotoxicity in SH-SY5Y neuroblastoma cells. Cell viability was assessed by MTT assay. Each bar represents mean  $\pm$  SEM of three independent experiments; \* $P < 0.05$ , \*\* $P < 0.01$ , \*\*\* $P < 0.001$  vs NMDA alone.

later stages of AD and on the other for developing new multipotent drug leads for the treatment of AD-type neurodegeneration.

## 5. Experimental section

### 5.1. Chemistry

Compounds **8a**, **9a**, **10a** and **16** were synthesized according to known procedures with slight modifications [28,29,39,40]; their

melting points and spectral data were in full agreement with those reported in literature, and no effort was made at this stage to optimize the yields. Unless otherwise stated, starting materials and all chemicals and solvents were purchased from Sigma-Aldrich. Melting points were determined by using the capillary method on a Stuart Scientific SMP3 electrothermal apparatus and are uncorrected. Final compound purities were assessed by elemental analyses (C, H, N), performed on Euro EA3000 analyzer (Eurovector, Milan, Italy) by the Analytical Laboratory Service of the Department of Pharmacy

–Drug Sciences of the University of Bari (Italy), and the results agreed to within  $\pm 0.40\%$  of theoretical values. Mass spectra were obtained by Agilent 1100 Series LC-MSD Trap System VL, equipped with ESI (electrospray ionization) source (Agilent Technologies Italia S.p.A., Cernusco sul Naviglio, Milan, Italy). The high resolution molecular masses of test compounds were assessed by Agilent 6530 Accurate Mass Q-TOF (Agilent Technologies Italia S.p.A., Cernusco sul Naviglio, Milan, Italy). IR spectra were recorded via KBr disks on a Perkin-Elmer Spectrum One Fourier transform infrared spectrophotometer (Perkin-Elmer Ltd., Buckinghamshire, U.K.), and the most significant absorption bands are listed.  $^1\text{H}$  NMR spectra were recorded at 300 MHz on a Varian Mercury 300 instrument. Chemical shifts are expressed in  $\delta$  and the coupling constants  $J$  are in hertz (Hz). The following abbreviations are used: s, singlet; d, doublet; dd, doublet-doublet; t, triplet; m, multiplet. Signals due to NH and OH protons were located by deuterium exchange with  $\text{D}_2\text{O}$ . Chromatographic separations were performed on silica gel 60 for column chromatography (Merck 70–230 mesh, or alternatively 15–40. mesh for flash chromatography).

Synthesis procedures, analytical and spectral data of **8a**, **9a**, **10a**, **11e**, **f**, **12b**, **13–16**, **20–22** are described below, whereas experimental details on synthesis, analysis and spectra of the other compounds (**8b**, **9b**, **10b**, **11a–d**, **12a**, **12c–i**, **14**, **17–19**) are reported in Supplementary material.

#### 5.1.1. 1,2,3,9-Tetrahydro-4H-carbazol-4-one (**8a**)

A solution of phenylhydrazine (0.9 mL, 8.92 mmol) in 10 mL of water was added dropwise to 1,3-cyclohexanedione (1.0 g, 8.92 mmol) in 50 mL of distilled water, and the solution was stirred overnight at room temperature. The precipitate was isolated by filtration, washed with 100 mL of water and dried, yielding 1.65 g (Yield 90%) of cyclohexane-1,3-dione phenylhydrazone (m.p. 176–178 °C; lit. 175–177 °C) [28,29,40], which was then refluxed in 15 mL of TFA for 24 h. After cooling, the solvent was removed under  $\text{N}_2$  gas stream and the residue was treated with 100 mL of water. Compound **8a** as a brown solid (1.30 g, yield 70%, crude) was isolated by filtration, washed with 100 mL of water, dried and used in the preparation of the corresponding oxime without further purification. Spectral data were in agreement with those of literature. IR (KBr,  $\text{cm}^{-1}$ ): 3162, 1610, 1580, 1460.  $^1\text{H}$  NMR (300 MHz,  $\text{CDCl}_3$ )  $\delta$  ppm 11.70 (s, br, 1H), 8.10–8.00 (m, 1H), 7.45–7.38 (m, 1H), 7.15–7.00 (m, 2H), 2.97 (t,  $J = 7.0$  Hz, 2H), 2.44 (t,  $J = 7.0$  Hz, 2H), 2.15 (quintet,  $J = 7.0$  Hz, 2H).

#### 5.1.2. 1,2,3,9-Tetrahydro-4H-carbazol-4-one oxime (**9a**)

Sodium acetate (1.33 g, 16.2 mmol) and hydroxylamine hydrochloride (1.13 g, 16.2 mmol) were added to **8a** (2.0 g, 10.8 mmol) in 30 mL of EtOH/water 2/1 v/v, and the mixture was refluxed 24 h under nitrogen atmosphere. After cooling, the solvent was removed and the residue was suspended in 150 mL of water and triturated, until precipitation of the desired oxime product as brown solid, which was collected by filtration and recrystallized from EtOH and water (1.73 g, Yield 80%). Analytical and spectral data were in agreement with those of literature (m.p. 205–9 °C, dec.) [29,40]. IR (KBr,  $\text{cm}^{-1}$ ): 3418, 3373, 1607, 1578, 1464, 1251, 1177, 753, 747.  $^1\text{H}$  NMR (300 MHz,  $\text{DMSO}-d_6$ )  $\delta$  ppm 11.22 (s, br, 1H) 10.26 (s, 1H), 7.92 (d,  $J = 8.0$  Hz, 1H), 7.34 (d,  $J = 8.0$  Hz, 1H), 7.10 (t,  $J = 8.0$  Hz, 1H), 7.03 (t,  $J = 8.0$  Hz, 1H), 2.82 (t,  $J = 6.5$  Hz, 2H), 2.70 (t,  $J = 6.5$  Hz, 2H), 1.94 (quintet,  $J = 6.5$  Hz, 2H).

#### 5.1.3. 3,4,5,6-Tetrahydroazepino [4,3-b]indol-1(2H)-one (**10a**)

Compound **9a** (2.5 g, 12.5 mmol) of was added portionwise to 95 g of preheated (110 °C) PPA under vigorous stirring, and the mixture was stirred at this temperature for 30 min. Then, 200 g of ice were carefully poured into the mixture and triturated until complete dissolution of PPA and formation of a grey precipitate, which was collected by filtration under reduced pressure, washed with 100 mL of water, 10 mL of 5% diluted ammonia and further 100 mL of water. The solid was then suspended into 50 mL of MeOH and, after addition of 1.0 g of vegetal carbon, refluxed for 1 h. After cooling, the suspension was filtered on a Celite pad and the solvent removed to furnish **10a** as pale brown solid (1.75 g, 70% Yield). Analytical and spectral data were in good agreement with those of literature [29,40]; m.p. 208–10 °C (lit. 209–211 °C). IR (KBr,  $\text{cm}^{-1}$ ): 3302, 1626, 1591, 1480.  $^1\text{H}$  NMR (300 MHz,  $\text{DMSO}-d_6$ )  $\delta$  ppm 11.45 (br, 1H), 8.23 (d,  $J = 8.0$  Hz, 1H), 7.43 (t,  $J = 7.0$  Hz, 1H), 7.32 (d,  $J = 8.0$  Hz, 1H), 7.11 (t,  $J = 8.0$  Hz, 1H), 7.04 (t,  $J = 8.0$  Hz, 1H), 3.24 (q,  $J = 7.0$  Hz, 2H), 3.14 (t,  $J = 7.0$  Hz, 2H), 2.10–2.00 (m, 2H).

#### 5.1.4. 6-Substituted derivatives of the

##### 3,4,5,6-tetrahydroazepino[4,3-b]indol-1(2H)-one

The preparation method of the *N*-phenethyl substituted compound **12b** is reported as a representative example of the synthesis procedures of **11a–d**, **12a–i**, **17** and **18**.

##### 5.1.4.1. 6-(2-Phenylethyl)-3,4,5,6-tetrahydroazepino[4,3-b]indol-1(2H)-one (**12b**)

TBAB (0.443 g, 1.38 mmol), phenethyl bromide (0.65 mL, 2.50 mmol) and 5.0 mL of 25% m/m NaOH solution were added to a solution of **10a** (0.25 g, 1.275 mmol) in 15 mL of dry DCM. The mixture was stirred at rt for 48 h, and then diluted with 20 mL of DCM and 20 mL of water. The collected organic phase was washed twice with 20 mL of brine, dried ( $\text{Na}_2\text{SO}_4$ ), filtered and concentrated under reduced pressure. The residue was purified by chromatography on silica gel, eluting with ethyl acetate, to afford **12b** as pale brown solid (0.270 g, 70% yield). m.p. 202–203 °C. IR (KBr,  $\text{cm}^{-1}$ ): 3265, 3173, 3026, 2919, 1633, 1528, 1461, 813, 745, 702.  $^1\text{H}$  NMR (300 MHz,  $\text{DMSO}-d_6$ )  $\delta$  ppm 8.23 (dd,  $J_1 = 2.5$  Hz,  $J_2 = 8.0$  Hz, 1H), 7.48 (d,  $J = 8.0$  Hz, 1H), 7.44 (t br,  $J = 5.5$  Hz, 1H), 7.30–7.00 (m, 7H), 4.32 (t,  $J = 7.0$  Hz, 2H), 3.10–3.00 (m, 2H), 2.96 (t,  $J = 7.0$  Hz, 2H), 2.77 (t,  $J = 7.0$  Hz, 2H), 1.95–1.80 (m, 2H).  $^{13}\text{C}$  NMR ( $\text{CDCl}_3$ ): 26.5, 27.0, 35.6, 41.4, 45.0, 106.1, 108.8, 121.6, 122.5, 122.7, 126.9, 128.3, 128.7 (2 C), 128.9 (2 C), 135.8, 138.0, 142.4, 169.1 HRMS (ESI)  $m/z$   $[\text{M}+\text{H}]^+$  calcd for  $\text{C}_{20}\text{H}_{21}\text{N}_2\text{O}^+$ , 305.1648; found, 305.1644. Anal. Calcd for  $\text{C}_{20}\text{H}_{20}\text{N}_2\text{O}$ : C, 78.92; H, 6.62; N, 9.20. Found: C, 79.05; H, 6.82; N, 9.33.

##### 5.1.4.2. 6-(3-Aminopropyl)-3,4,5,6-tetrahydroazepino[4,3-b]indol-1(2H)-one (**11e**)

$\text{NaBH}_4$  (0.223 g, 5.90 mmol) was added portionwise to a cooled (0 °C) solution of **11d** (0.150 g, 0.59 mmol) and  $\text{CoCl}_2 \times 6\text{H}_2\text{O}$  (0.280 g, 1.18 mmol) in 15 mL of methanol, and the mixture was stirred 1 h at rt. After quenching with 10 mL of 3 N HCl, the solution was stirred at rt until disappearance of precipitate, and then concentrated under reduced pressure. The residue was suspended in 20 mL of water, and 2 N NaOH was added to alkaline pH. The obtained aqueous suspension was extracted with DCM (3  $\times$  20 mL), and the collected organic phases were dried ( $\text{Na}_2\text{SO}_4$ ), filtered and concentrated, to yield **11e** as brown oil (0.10 g, Yield 66%). IR (KBr,  $\text{cm}^{-1}$ ):



3343, 3261, 1627, 1523, 1465, 783, 754.  $^1\text{H}$  NMR (300 MHz, DMSO- $d_6$ )  $\delta$  ppm 8.21 (d,  $J = 8.0$  Hz, 1H), 7.60 (s br, 1H), 7.53 (d,  $J = 8.0$  Hz, 1H), 7.15 (t,  $J = 7.0$  Hz, 1H), 7.07 (t,  $J = 7.0$  Hz, 1H), 4.26 (t,  $J = 7.5$  Hz, 2H), 3.21–3.16 (m, 2H), 3.07 (t,  $J = 6.5$  Hz, 2H), 2.89–2.80 (m, 2H), 2.65 (s, br, 2H), 2.05–1.90 (m, 4H). MS (ESI)  $m/z$   $[\text{M}+\text{H}]^+$  258.

#### 5.1.4.3. Ethyl

##### 3-(1-oxo-2,3,4,5-tetrahydroazepino[4,3-b]indol-6(1H)-yl)propylcarbamate (11f)

Triethylamine (0.2 mL, 1.6 mmol) and, dropwise, ethyl chloroformate (0.1 mL, 0.8 mmol) were added to a solution of **7e** (0.10 mg, 0.4 mmol) in 15 mL of dry THF. The mixture was stirred overnight at rt and, after solvent removal, the residue was partitioned between 50 mL of ethyl acetate and 20 mL of brine. The organic phase was dried ( $\text{Na}_2\text{SO}_4$ ), filtered and concentrated under reduced pressure, and the obtained residue was recrystallized from ethyl acetate to leave **11f** as white solid (0.08 g, Yield 60%). m.p. 134–135 °C. IR (KBr,  $\text{cm}^{-1}$ ): 3266, 3173, 3023, 2979, 1718, 1623, 1525, 1246, 1042, 781, 763.  $^1\text{H}$  NMR (300 MHz, DMSO- $d_6$ )  $\delta$  ppm 8.21 (d,  $J = 7.0$  Hz, 1H), 7.48 (t,  $J = 5.0$  Hz, 1H), 7.42 (d,  $J = 8.0$  Hz, 1H), 7.24 (t,  $J = 5.0$  Hz, 1H), 7.13 (t,  $J = 7.0$  Hz, 1H), 7.07 (t,  $J = 7.0$  Hz, 1H), 4.13 (t,  $J = 7.0$  Hz, 2H), 3.99 (q,  $J = 7.0$  Hz, 2H), 3.16 (dd,  $J_1 = 3.0$  Hz,  $J_2 = 5.0$  Hz, 2H), 3.10–2.95 (m, 4H), 2.10–1.95 (m, 2H), 1.78 (quintet,  $J = 7.0$  Hz, 2H). HRMS (ESI)  $m/z$   $[\text{M}+\text{H}]^+$  calcd for  $\text{C}_{18}\text{H}_{24}\text{N}_3\text{O}_3^+$ , 330.1812; found, 330.1808. Anal. Calcd for  $\text{C}_{18}\text{H}_{23}\text{N}_3\text{O}_3$ : C, 65.63; H, 7.04; N, 12.76. Found: C, 65.70; H, 7.22; N, 12.78.

##### 5.1.4.4. 2-Methyl-6-(2-phenylethyl)-3,4,5,6-tetrahydroazepino[4,3-b]indol-2(1H)-one (13)

NaH in 60% mineral oil dispersion (0.02 g) was added to a solution of **12b** (0.08 g, 0.26 mmol) in 3 mL of anhydrous DMF. After 10 min of stirring at rt,  $\text{CH}_3\text{I}$  (0.1 mL, 1.5 mmol) was added, and the mixture was stirred at rt overnight, whereupon further 20 mg of NaH and 0.1 mL of  $\text{CH}_3\text{I}$  were added, and stirring prolonged for 6 h until disappearance of the starting material (TLC). The mixture was diluted with 50 mL of water and aqueous phase was extracted with  $3 \times 15$  mL of ethyl acetate. The collected organic phases were dried ( $\text{Na}_2\text{SO}_4$ ), filtered and concentrated under reduced pressure. The oil residue was purified by chromatography on silica gel (ethyl acetate/*n*-hexane 95/5 v/v) to afford compound **13** as pale brown oil (0.03 g, Yield 36%). IR (KBr,  $\text{cm}^{-1}$ ): 2918, 1632, 1525, 1458, 810, 747, 700.  $^1\text{H}$  NMR (300 MHz, DMSO- $d_6$ )  $\delta$  ppm 8.20 (dd,  $J_1 = 2.5$  Hz,  $J_2 = 8.0$  Hz, 1H), 7.47 (d,  $J = 8.0$  Hz, 1H), 7.42 (t br,  $J = 5.5$  Hz, 1H), 7.28–7.00 (m, 7H), 4.33 (t,  $J = 7.0$  Hz, 2H), 3.12 (s, 3H), 3.10–3.00 (m, 2H), 2.94 (t,  $J = 7.0$  Hz, 2H), 2.79 (t,  $J = 7.0$  Hz, 2H), 1.95–1.80 (m, 2H). HRMS (ESI)  $m/z$   $[\text{M}+\text{H}]^+$  calcd for  $\text{C}_{21}\text{H}_{23}\text{N}_2\text{O}^+$ , 319.1805; found, 319.1802. Anal. Calcd for  $\text{C}_{21}\text{H}_{22}\text{N}_2\text{O}$ : C, 79.21; H, 6.96; N, 8.80. Found: C, 79.45; H, 7.04; N, 8.79.

##### 5.1.4.5. 6-(2-Phenylethyl)-1,2,3,4,5,6-hexahydroazepino[4,3-b]indole hydrochloride (14)

$\text{LiAlH}_4$  (0.127 g, 3.33 mmol) was added to a solution of **12b** (0.145 g, 0.48 mmol) in 20 mL of dry dioxane, and the mixture was refluxed until disappearance of the starting material (TLC). After cooling, the reaction was quenched by adding 10 mL of a saturated solution of sodium sulfate ( $\text{Na}_2\text{SO}_4$ ) and stirred at rt for 30 min. The mixture was then filtered and the precipitate was washed with 20 mL of dioxane. The collected filtrates were concentrated and the residue,

suspended in 50 mL of distilled water, was extracted with  $3 \times 50$  mL of  $\text{CHCl}_3$ . The organic fractions were dried ( $\text{Na}_2\text{SO}_4$ ), filtered and concentrate under reduced pressure, and the oil residue was dissolved in 5 mL of 1.25 M HCl methanolic solution and stirred at rt for 4 h. After solvent removal, the solid residue was recrystallized from ethyl acetate and few drops of ethanol, to afford compound **14**-HCl salt as dark brown solid (0.070 g, Yield 50%). m.p. 241–242 °C. IR (KBr,  $\text{cm}^{-1}$ ): 3230, 1520, 1460, 810, 742, 700.  $^1\text{H}$  NMR (300 MHz, DMSO- $d_6$ )  $\delta$  ppm 9.17 (s, 2H), 7.56 (d,  $J = 7.0$  Hz, 1H), 7.44 (d,  $J = 8.0$  Hz, 1H), 7.39–7.08 (m, 6H), 7.07 (t,  $J = 8.5$  Hz, 2H), 4.45–4.25 (m, 4H), 3.40–3.25 (m, 2H), 2.95–2.75 (m, 4H), 1.95–1.75 (m, 2H).  $^{13}\text{C}$  NMR ( $\text{CDCl}_3$ ): 25.4, 26.5, 31.6, 42.2, 42.8, 46.0, 110.1, 120.9, 121.9, 122.5, 122.7, 126.7, 128.0, 128.3 (2 C), 128.5 (2 C), 135.0, 137.3, 139.2 HRMS (ESI)  $m/z$   $[\text{M}+\text{H}]^+$  calcd for  $\text{C}_{20}\text{H}_{23}\text{N}_2^+$ , 291.1856; found, 291.1852. Anal. Calcd for  $\text{C}_{20}\text{H}_{23}\text{ClN}_2 \times \text{H}_2\text{O}$ : C, 69.63; H, 7.31; N, 8.12. Found: C, 69.85; H, 7.54; N, 8.09.

##### 5.1.4.6. N-[(4-Methylphenyl)sulfonyl]oxy-1,2,3,9-tetrahydro-4H-carbazol-4-ylidene (15)

DMAP (1.83 g, 15.0 mmol) and, dropwise, a solution of tosyl chloride (1.05 g, 15.0 mmol) in 10 mL of dry DCM were added to a solution of **9a** (1.00 g, 5 mmol) in 15 mL of dry DCM cooled at 0 °C. The mixture was stirred at rt under  $\text{N}_2$  atmosphere for 48 h. The reaction mixture was then washed with 1 N HCl ( $3 \times 20$  mL) and brine ( $3 \times 20$  mL), dried ( $\text{Na}_2\text{SO}_4$ ), filtered and concentrated under reduced pressure, to afford the desired product **15** (0.625 g, Yield 70%), whose analytical data were in good agreement with those of literature [29]; m.p. 138 °C (lit. 135–138 °C).  $^1\text{H}$  NMR (300 MHz, DMSO- $d_6$ )  $\delta$  ppm 10.16 (s, 1H), 7.92 (d,  $J = 8.0$  Hz, 1H), 7.82 (d,  $J = 8.5$  Hz, 2H), 7.34 (d,  $J = 8.0$  Hz, 1H), 7.28 (d,  $J = 8.5$  Hz, 2H), 7.08 (t,  $J = 8.0$  Hz, 1H), 7.02 (t,  $J = 8.0$  Hz, 1H), 2.82 (t,  $J = 6.5$  Hz, 1H), 2.70 (t,  $J = 6.5$  Hz, 1H), 2.33 (s, 3H), 1.94 (quintet,  $J = 6.5$  Hz, 2H). MS (ESI)  $m/z$   $[\text{M}+\text{H}]^+$  355.

##### 5.1.4.7. 3,4,5,6-Tetrahydroazepino[3,2-b]indol-2(1H)-one (16)

Compound **15** (1.37 g, 3.86 mmol) dissolved in 25 mL of chloroform was added to 60 g of  $\text{Al}_2\text{O}_3$ , previously activated with hexane, in 100 mL of toluene, and the suspension was stirred at rt for 48 and then refluxed for 8 h. After cooling, the heterogeneous mixture was filtered and the filtrate concentrated under reduced pressure, to yield the desired product **16** (0.230 g, Yield 30%), whose analytical data were in good agreement with those of literature [29]; m.p. 245 °C (lit. 243–244 °C). IR (KBr,  $\text{cm}^{-1}$ ): 3261, 3190, 1648, 783, 754.  $^1\text{H}$  NMR (300 MHz, DMSO- $d_6$ )  $\delta$  ppm 10.64 (s, 1H), 9.40 (s, 1H), 7.67 (d,  $J = 7.5$  Hz, 1H), 7.17 (d,  $J = 8.0$  Hz, 1H), 7.00 (t,  $J = 8.0$  Hz, 1H), 6.88 (t,  $J = 8.0$  Hz, 1H), 2.94 (t,  $J = 6.5$  Hz, 2H), 2.43 (t,  $J = 6.5$  Hz, 2H), 2.05–1.95 (m, 2H). MS (ESI): 223 ( $\text{M}+\text{Na}$ ) $^+$ .

##### 5.1.4.8. Methyl 1-(2-phenylethyl)-1H-indole-3-carboxylate (21)

NaH (0.10 g, 4.17 mmol) was added to a solution of methyl indole-3-carboxylate (0.50 g, 2.86 mmol) in 10 mL of dry DMF. After 10 min of stirring at rt, a solution of phenethyl bromide (0.50 mL, 3.43 mmol) in 5 mL of dry DMF was added dropwise, and the mixture was stirred at rt for 24 h. The reaction mixture was then poured into 200 mL of water, and the aqueous suspension was extracted with  $3 \times 30$  mL of ethyl acetate. The collected organic phases were dried ( $\text{Na}_2\text{SO}_4$ ), filtered and concentrated under reduced pressure, and the oil residue was purified by chromatography on silica gel, using ethyl acetate as the eluent, to afford **20** as white solid (0.250 g, Yield 46%). m.p. 103–105 °C. IR (KBr,  $\text{cm}^{-1}$ ): 1696, 1535, 1267, 1225, 1154,

1096, 775, 752, 738, 703.  $^1\text{H}$  NMR (300 MHz, DMSO- $d_6$ )  $\delta$  ppm 7.66 (s, 1H), 7.40–7.20 (m, 7H), 7.07 (dd,  $J_1 = 1.5$  Hz,  $J_2 = 7.5$  Hz, 1H), 4.37 (t,  $J = 7.0$  Hz, 2H), 3.89 (s, 3H), 3.17 (t,  $J = 8.0$  Hz, 2H). MS (ESI): 302 (M+Na) $^+$ .

#### 5.1.4.9. 1-(2-Phenylethyl)-1H-indole-3-carboxylic acid (**21**)

10 mL of 4 N NaOH was added to a solution of **20** (1.0 g, 3.58 mmol) in 20 mL of methanol, and the reaction mixture was stirred overnight at rt. After concentration under reduced pressure the aqueous suspension was acidified to pH 2, and then extracted with 3  $\times$  20 mL of ethyl acetate. The collected organic phases were dried (Na<sub>2</sub>SO<sub>4</sub>), filtered and concentrated under reduced pressure, to yield **21** as colorless oil (0.550 g, Yield 60%). IR (KBr, cm<sup>-1</sup>): 3025, 2933, 1661, 1525, 1275, 1177, 748, 698.  $^1\text{H}$  NMR (300 MHz, DMSO- $d_6$ )  $\delta$  ppm 10.00 (s, 1H), 7.70 (s, 1H), 7.30–7.00 (m, 9H), 4.25 (t,  $J = 7.0$  Hz, 2H), 3.13 (t,  $J = 7.0$  Hz, 2H). MS (ESI): 264 (M-H) $^-$ .

#### 5.1.4.10. 1-(2-Phenylethyl)-N-propyl-1H-indole-3-carboxamide (**22**)

DCC (230 mg, 1.12 mmol) and HOBt (0.152 g, 1.12 mmol) were added to a solution of **21** (0.300 g, 1.12 mmol) in 10 mL of dry DCM. After 30 min of stirring at rt, *n*-propylamine (0.1 mL, 1.12 mmol) was added and the reaction mixture was stirred at rt overnight and then filtered. The organic phase was washed twice with 10% m/m Na<sub>2</sub>CO<sub>3</sub>, 1 N HCl and brine, dried (Na<sub>2</sub>SO<sub>4</sub>), filtered and concentrated under reduced pressure. The oil residue was purified by chromatography on silica gel (eluent: 80% ethyl acetate/20% methanol v/v) to afford **22** as white solid (0.150 g, Yield 45%). m.p. 98–100 °C. IR (KBr, cm<sup>-1</sup>): 3383, 1627, 1541, 1223, 740, 695.  $^1\text{H}$  NMR (300 MHz, DMSO- $d_6$ )  $\delta$  7.95 (t,  $J = 7.0$  Hz, 1H), 7.50 (s, 1H), 7.35–7.20 (m, 5H), 7.07 (dd,  $J_1 = 8.0$  Hz,  $J_2 = 2.0$  Hz, 2H), 5.87 (s br, 1H), 4.36 (t,  $J = 7.0$  Hz, 2H), 3.45 (q,  $J = 7.0$  Hz, 2H), 3.12 (t,  $J = 7.5$  Hz, 2H), 1.69 (quintet,  $J = 6.0$  Hz, 2H), 1.01 (t,  $J = 7.5$  Hz, 3H). HRMS (ESI)  $m/z$  [M+H] $^+$  calcd for C<sub>20</sub>H<sub>23</sub>N<sub>2</sub>O $^+$  307.1805; found, 307.1800 Anal. Calcd for C<sub>20</sub>H<sub>22</sub>N<sub>2</sub>O·1/4 H<sub>2</sub>O: C, 77.25; H, 7.29; N, 9.10. Found: C, 77.37; H, 7.43; N, 9.29.

## 5.2. Cholinesterase inhibition assay

The test compounds were assayed for their inhibitory activity toward AChE and BChE from electric eel and horse serum, respectively, and human cholinesterases as well (Sigma-Aldrich), following the Ellman's method [30]. The BChE activity was determined in a reaction mixture containing 100  $\mu\text{L}$  of a solution of BChE (0.9 U/mL in 0.1 M pH 8.0 phosphate buffer, PB), 100  $\mu\text{L}$  of a solution of 5,5-dithio-bis-(2-nitrobenzoic) acid (DTNB 3.3 mM in 0.1 M pH 7.0 PB, containing 0.1 mM NaHCO<sub>3</sub>), 100  $\mu\text{L}$  of a solution of the test compound (five to seven concentrations, ranging from  $1 \times 10^{-4}$  to  $1 \times 10^{-9}$  M in 0.1 M pH 8.0 PB), and 600  $\mu\text{L}$  of pH 8.0 PB. After incubation for 20 min at 25 °C, butyrylthiocholine iodide (100  $\mu\text{L}$  of 0.05 mM water solution) was added as the substrate, and the hydrolysis rates of the substrate monitored at 412 nm for 5.0 min at 25 °C. The concentration of compound which produced 50% inhibition of the BChE activity (IC<sub>50</sub>) was calculated by nonlinear regression of the response/concentration (log) curve, by using Prism GraphPad software (vers. 5.01). AChE inhibitory activity was determined similarly, by using a solution of AChE (0.415 U/mL in 0.1 M pH 8.0 PB), and acetylthiocholine iodide (0.05 mM) as the substrate. The inhibition data are reported as means of IC<sub>50</sub>'s determined at least in three independent measurements. To determine the type of inhibition for the most potent BuChE inhibitor **12d**, the Lineweaver-Burk eq (1/v

vs 1/[S]) was fitted for varying concentrations of substrates (25–250  $\mu\text{M}$ ) in the absence or presence of inhibitor at four different concentrations, ranging from 0.5 to 5.0 nM, and by using fixed amounts of enzymes (0.09 U  $\times$  mL<sup>-1</sup>). Replotting the slopes of the above plots against the inhibitor **12d** concentration (0 nM,  $r^2 = 0.9988$ ; 0.5 nM,  $r^2 = 0.9837$ ; 2.0 nM,  $r^2 = 0.9840$ ; 5.0 nM,  $r^2 = 0.9833$ ) yielded the K<sub>i</sub> value as the X-axis intercept.

## 5.3. Cell cultures and treatment

The human neuroblastoma SH-SY5Y, the human glioblastoma U-87, the human breast carcinoma MCF-7, and the human liver hepatocellular carcinoma HepG2 cell lines were purchased from ATCC. Cells were maintained in Dulbecco's modified Eagle's medium (DMEM) supplemented with 10% fetal bovine serum (FBS), 2 mM L-glutamine, 50 U/mL penicillin and 50  $\mu\text{g}/\text{mL}$  streptomycin in a humid atmosphere of 95% air and 5% CO<sub>2</sub> at 37 °C, and grown to 80% of confluence. Prior to cell treatment, the medium was replaced with fresh medium containing test compounds in the range 0.1–500  $\mu\text{M}$  on U-87, MCF-7 and HepG2 cells. Toxicity studies on SH-SY5Y cells were carried out using a reduced serum medium (2% FBS), and the test compounds were prepared as a stock solution of 20 mM in DMSO and were used at concentrations ranging from 0.1 to 1000  $\mu\text{M}$ . In the cytoprotection assay, SH-SY5Y cells were co-incubated with NMDA at a concentration of 250  $\mu\text{M}$  and test compounds at six different concentrations (0.1–50  $\mu\text{M}$ ).

## 5.4. Cell viability

The number of living cells was evaluated by the 3-(4,5-dimethylthiazol-2-yl)-2,5-diphenyltetrazolium bromide (MTT) assay. Briefly, 100  $\mu\text{L}$  of cell suspension were plated in 96-well plates at a density of ~5000 cells/well. After 1 day incubation at 37 °C in a humid atmosphere with 5% CO<sub>2</sub>, the culture medium was replaced with 150  $\mu\text{L}$  of fresh medium or medium containing different concentrations of the test compounds. Untreated cells were used as positive control and cells incubated with a 2% (w/v) SDS solution were used as negative control. After the incubation period of 48 h, 10  $\mu\text{L}$  of a 0.5% (w/v) MTT/PBS solution were added to each well and the incubation was prolonged further for 4 h. After this period, medium was removed and replaced with 150  $\mu\text{L}$  of a DMSO/ethanol (1/1 v/v) solution per well. The absorbance of the individual well was measured by a microplate reader (Wallac Victor3, 1420 Multilabel Counter, Perkin-Elmer). Each compound concentration was tested in triplicate, and results presented as percentage of the control value.

For the neuroprotection assay, SH-SY5Y cells were seeded in 96-well plates at the same density used for cytotoxicity assay. Cells were exposed for 48 h to NMDA at a final concentration of 250  $\mu\text{M}$  in reduced-serum medium in the absence or presence of test compounds at concentrations ranging from 0.1 to 50  $\mu\text{M}$  at 37 °C. Cell viability was also measured by the MTT assay.

Data are presented as the mean  $\pm$  SEM. Statistical comparisons were performed by one-way ANOVA followed by multiple comparison tests (Dunnett's test) using the statistical package in the GraphPad Prism software vers. 5.01; values of  $P < 0.05$  were considered statistically significant.

## Author contributions

M.d.C., G.Z., M.M. and S.C. contributed to chemistry and performed enzymes' inhibition measurements. N.D. and D.T. carried out

cytotoxicity assays and biological data analysis. C.D.A. and M.d.C. designed the research project and interpreted SAR data. All the authors approved the final version of the manuscript.

### Conflict of interest

We declare that we have no conflict of interest.

### Acknowledgements

The financial support from MIUR, Italy (Grant PRIN 2009ESXPT2\_005) is gratefully acknowledged.

### Appendix A. Supplementary data

Supplementary data related to this article can be found at <http://dx.doi.org/10.1016/j.ejmech.2016.09.037>.

### References

- [1] A. Kumar, A. Singh, A. Ekavali, A review on Alzheimer's disease pathophysiology and its management: an update, *Pharmacol. Rep.* 67 (2015) 195–203.
- [2] W.J. Geldenhuys, A.S. Darvesh, Pharmacotherapy of Alzheimer's disease: current and future trends, *Expert Rev. Neurother.* 15 (2015) 3–5.
- [3] E. Giacobini, Cholinesterase inhibitors stabilize Alzheimer's disease, *Ann. N. Y. Acad. Sci.* 920 (2006) 321–327.
- [4] E. Simoni, S. Daniele, G. Bottegoni, D. Pizzirani, M.L. Trincavelli, L. Goldoni, G. Tarozzo, A. Reggiani, C. Martini, D. Piomelli, C. Melchiorre, M. Rosini, A. Cavalli, Combining galantamine and memantine in multitargeted, new chemical entities potentially useful in Alzheimer's disease, *J. Med. Chem.* 55 (2012) 9708–9721.
- [5] M. Rosini, E. Simoni, A. Minarini, C. Melchiorre, Multi-target design strategies in the context of Alzheimer's disease: acetylcholinesterase inhibition and NMDA receptor antagonism as the driving forces, *Neurochem. Res.* 39 (2014) 1914–1923.
- [6] C.G. Zhan, F. Zheng, D.W. Landry, Fundamental reaction mechanism for cocaine hydrolysis in human butyrylcholinesterase, *J. Am. Chem. Soc.* 125 (2003) 2462–2474.
- [7] P. Masson, E. Carletti, F. Nachon, Structure, activities and biomedical applications of human butyrylcholinesterase, *Protein Pept. Lett.* 16 (2009) 1215–1224.
- [8] N.H. Greig, T. Utsuki, D.K. Ingram, Y. Wang, G. Pepeu, C. Scali, Q.S. Yu, J. Mamezcarz, H.W. Holloway, T. Giordano, D. Chen, K. Furukawa, K. Sambamurti, A. Brossi, D.K. Lahiri, Selective butyrylcholinesterase inhibition elevates brain acetylcholine, augments learning and lowers Alzheimer  $\beta$ -amyloid peptide in rodent, *Proc. Natl. Acad. Sci. U. S. A.* 102 (2005) 17213–17218.
- [9] C. Geula, S. Darvesh, Butyrylcholinesterase, cholinergic neurotransmission and the pathology of Alzheimer's disease, *Drugs Today (Barc)* 40 (2004) 711–721.
- [10] S. Darvesh, M.K. Cash, G.A. Reid, E. Martin, A. Mitnitski, C. Geula, Butyrylcholinesterase is associated with  $\beta$ -amyloid plaques in the transgenic APPSWE/PSEN1dE9 mouse model of Alzheimer disease, *J. Neuropathol. Exp. Neurol.* 71 (2012) 2–14.
- [11] C. Galdeano, E. Viayna, P. Arroyo, A. Bidon-Chanal, J.R. Blas, D. Muñoz-Torero, F.J. Luque, Structural determinants of the multifunctional profile of dual binding site acetylcholinesterase inhibitors as anti-Alzheimer agents, *Curr. Pharm. Des.* 16 (2010) 2818–2836.
- [12] E.G. Duysen, B. Li, S. Darvesh, O. Lockridge, Sensitivity of butyrylcholinesterase knockout mice to (-)-huperzine A and donepezil suggests humans with butyrylcholinesterase deficiency may not tolerate these Alzheimer's disease drugs and indicates butyrylcholinesterase function in neurotransmission, *Toxicology* 233 (2007) 60–69.
- [13] (a) Q. Yu, H.W. Holloway, T. Utsuki, A. Brossi, N.H. Greig, Synthesis of novel phenserine-based-selective inhibitors of butyrylcholinesterase for Alzheimer's disease, *J. Med. Chem.* 42 (1999) 1855–1861; (b) J. Takahashi, I. Hijikuro, T. Kihara, M.G. Muruges, S. Fuse, R. Kunimoto, Y. Tsumura, A. Akaike, T. Niidome, Y. Okuno, T. Takahashi, H. Sugimoto, Design, synthesis, evaluation and QSAR analysis of N(1)-substituted norcymserine derivatives as selective butyrylcholinesterase inhibitors, *Bioorg. Med. Chem. Lett.* 20 (2010) 1718–1720; (c) J. Takahashi, I. Hijikuro, T. Kihara, M.G. Muruges, S. Fuse, Y. Tsumura, A. Akaike, T. Niidome, T. Takahashi, H. Sugimoto, Design, synthesis and evaluation of carbamate-modified (-)-N(1)-phenethylmorphostigmine derivatives as selective butyrylcholinesterase inhibitors, *Bioorg. Med. Chem. Lett.* 20 (2010) 1721–1723; (d) M. Shinada, F. Narumi, Y. Osada, K. Matsumoto, T. Yoshida, K. Higuchi, T. Kawasaki, H. Tanaka, Synthesis of phenserine analogues and evaluation of their cholinesterase inhibitory activities, *Bioorg. Med. Chem.* 20 (2012) 4901–4914.
- [14] (a) G. Sinko, Z. Kovarik, E. Reiner, V. Simeon-Rudolf, J. Stojan, Mechanism of stereoselective interaction between butyrylcholinesterase and ethopropazine enantiomers, *Biochimie* 93 (2011) 1797–1807; (b) S. Darvesh, K.V. Darvesh, R.S. McDonald, D. Mataija, R. Walsh, S. Mothana, O. Lockridge, E. Martin, Carbamates with differential mechanism of inhibition toward acetylcholinesterase and butyrylcholinesterase, *J. Med. Chem.* 51 (2008) 4200–4212; (c) G.C. González-Muñoz, M.P. Arce, B. López, C. Pérez, A. Romero, L. del Barrio, M.D. Martín-de-Saavedra, J. Egea, R. León, M. Villarroya, M.G. López, A.G. García, S. Conde, M.I. Rodríguez-Franco, N-acylaminophenothiazines: neuroprotective agents displaying multifunctional activities for a potential treatment of Alzheimer's disease, *Eur. J. Med. Chem.* 46 (2011) 2224–2235.
- [15] (a) M. Decker, F. Krauth, J. Lehmann, Novel tricyclic quinazolinimines and related tetracyclic nitrogen bridgehead compounds as cholinesterase inhibitors with selectivity towards butyrylcholinesterase, *Bioorg. Med. Chem.* 14 (2006) 1966–1977; (b) M. Decker, Homobivalent quinazolinimines as novel nanomolar inhibitors of cholinesterases with dirigible selectivity toward butyrylcholinesterase, *J. Med. Chem.* 49 (2006) 5411–5413; (c) X. Chen, I.G. Tikhonova, M. Decker, Probing the mid-gorge of cholinesterases with spacer-modified bivalent quinazolinimines leads to highly potent and selective butyrylcholinesterase inhibitors, *Bioorg. Med. Chem.* 19 (2011) 1222–1235.
- [16] M. Bajda, A. Wieckowska, M. Hebda, N. Guziar, C.A. Sottrifer, B. Malawska, Structure-based search for new inhibitors of cholinesterases, *Int. J. Mol. Sci.* 14 (2013) 5608–5632.
- [17] P. Masson, M.T. Froment, C.F. Bartels, O. Lockridge, Asp70 in the peripheral anionic site of human butyrylcholinesterase, *Eur. J. Biochem.* 235 (1996) 36–48.
- [18] Y. Nicolet, O. Lockridge, P. Masson, J.C. Fontecilla-Camps, F. Nachon, Crystal structure of human butyrylcholinesterase and of its complexes with substrate and products, *J. Biol. Chem.* 278 (2003) 41141–41147.
- [19] (a) S.Y. Chiou, T.T. Weng, G.Z. Lin, R.J. Lu, S.Y. Jian, G. Lin, Molecular docking of different inhibitors and activators to butyrylcholinesterase, *J. Biomol. Struct. Dyn.* 33 (2014) 563–572.
- [20] F.H. Darras, B. Kling, J. Heilmann, M. Decker, Neuroprotective tri- and tetracyclic BChE inhibitors releasing reversible inhibitors upon carbamate transfer, *ACS Med. Chem. Lett.* 3 (2012) 914–919.
- [21] L.G. Voskressensky, T.N. Borisova, L.N. Kulikova, A.V. Varlamov, M. Catto, C. Altomare, A. Carotti, Tandem cleavage of hydrogenated  $\beta$ - and  $\gamma$ -Carbolines - new practical synthesis of tetrahydroazocino[4,5-b]indoles and tetrahydroazocino[5,4-b]indoles showing acetylcholinesterase inhibitory activity, *Eur. J. Org. Chem.* 14 (2004) 3128–3135.
- [22] A. Carotti, M. de Candia, M. Catto, T.N. Borisova, A.V. Varlamov, E. Méndez-Alvarez, R. Soto-Otero, L.G. Voskressensky, C. Altomare, Ester derivatives of annulated tetrahydroazocines: a new class of selective acetylcholinesterase inhibitors, *Bioorg. Med. Chem.* 14 (2006) 7205–7212.
- [23] R.W. Jones, Dimebon disappointment, *Alzheimers Res. Ther.* 2 (2010) 25.
- [24] (a) V.V. Grigorev, O.A. Dranyi, S.O. Bachurin, Comparative study of action mechanisms of dimebon and memantine on AMPA- and NMDA-subtypes glutamate receptors in rat cerebral neurons, *Bull. Exp. Biol. Med.* 136 (2003) 474–477; (b) J. Wang, M.G. Ferruzzi, M. Varghese, X. Qian, A. Cheng, M. Xie, W. Zhao, L. Ho, G.M. Pasinetti, Preclinical study of dimebon on  $\beta$ -amyloid-mediated neuropathology in Alzheimer's disease, *Mol. Neurodegener.* 6 (2011) 7 (10 pages).
- [25] S. Bachurin, E. Bukatina, N. Lermontova, S. Tkachenko, A. Afanasiev, V. Grigoriev, I. Grigorieva, Y. Ivanov, S. Sablin, N. Zefirov, Antihistamine agent dimebon as a novel neuroprotector and a cognition enhancer, *Ann. N.Y. Acad. Sci.* 939 (2006) 425–435.
- [26] M. Giorgetti, J.A. Gibbons, S. Bernales, I.E. Alfaro, C. Drieu La Rochelle, T. Cremers, C.A. Altar, R. Wronski, B. Hutter-Paier, A.A. Protter, Cognition-enhancing properties of dimebon in a rat novel object recognition task are unlikely to be associated with acetylcholinesterase inhibition or N-methyl-D-aspartate receptor antagonism, *J. Pharmacol. Exp. Ther.* 333 (2010) 748–757.
- [27] M. Rosini, E. Simoni, M. Bartolini, E. Soriano, J.M. Contelles, V. Andrisano, B. Monti, M. Windisch, B. Hutter-Paier, D.W. McClymont, I.R. Mellor, M.L. Bolognesi, The bivalent ligand approach as a tool for improving the in vitro anti-Alzheimer multitarget profile of dimebon, *ChemMedChem* 8 (2013) 1276–1281.
- [28] L.G. Voskressensky, S.V. Akbulatov, T.N. Borisova, A.V. Varlamov, A novel synthesis of hexahydroazonoindoles using activated alkynes in an azepine ring expansion, *Tetrahedron* 62 (2006) 12392–12397.

- [29] J.B. Hester, Azepinoindoles. II. 1,2,3,4,5,6-Hexahydroazepino[3,2-b]indole and 1,2,3,4,5,6-hexahydroazepino[4,3-b]indole, *J. Org. Chem.* 32 (1967) 3804–3808.
- [30] G.L. Ellman, K.D. Courtney, V. Andres, R.M. Feather-Stone, A new and rapid colorimetric determination of acetylcholinesterase activity, *Biochem. Pharmacol.* 7 (1961) 88–95.
- [31] D.E. Moore, G.P. Hess, Acetylcholinesterase-catalyzed hydrolysis of an amide, *Biochemistry* 14 (1975) 2386–2389.
- [32] C. Bissantz, B. Kuhn, M. Stahl, A medicinal Chemist's guide to molecular interactions, *J. Med. Chem.* 53 (2010) 5061–5084.
- [33] M.J. Oset-Gasque, M.P. González, J. Pérez-Peña, N. García-Font, A. Romero, J. del Pino, E. Ramos, D. Hadjipavlou-Litina, E. Soriano, M. Chioua, A. Samadi, D.S. Raghuvanshi, K.N. Singh, J. Marco-Contelles, Toxicological and pharmacological evaluation, antioxidant, ADMET and molecular modeling of selected racemic chromenotacrine {11-amino-12-aryl-8,9,10,12-tetrahydro-7H-chromeno[2,3-b]quinolin-3-ols} for the potential prevention and treatment of Alzheimer's disease, *Eur. J. Med. Chem.* 74 (2014) 491–501.
- [34] C. Klein, C. Patte-Mensah, O. Taleb, J.J. Bourguignon, M. Schmitt, F. Bihel, M. Maitre, A.G. Mensah-Nyagan, The neuroprotector kynurenic acid increases neuronal cell survival through neprilysin induction, *Neuropharmacology* 70 (2013) 254–260.
- [35] T. Lee, H. Heo, Y. Kim Kwon, Effect of berberine on cell survival in the developing rat brain damaged by MK-801, *Exp. Neurobiol.* 19 (2010) 140–145.
- [36] D. Jantas, M. Pytel, J.W. Mozrzyms, M. Leskiewicz, M. Regulska, L. Antkiewicz-Michaluk, W. Lason, The attenuating effect of memantine on staurosporine-, salsolinol- and doxorubicin-induced apoptosis in human neuroblastoma SH-SY5Y cells, *Neurochem. Int.* 52 (2008) 864–877.
- [37] E. Marutani, S. Kosugi, K. Tokuda, A. Khatri, R. Nguyen, D.N. Atochin, K. Kida, K. Van Leyen, K. Arai, F. Ichinose, A novel hydrogen sulfide-releasing N-methyl-d-aspartate receptor antagonist prevents ischemic neuronal death, *J. Biol. Chem.* 287 (2012) 32124–32135.
- [38] W.F. Van den Hof, M.L. Coonen, M. van Herwijnen, K. Brauers, W.K. Wodzig, J.H. van Delft, J.C. Kleinjans, *Chem. Res. Toxicol.* 27 (2014) 433–442.
- [39] (a) X. Li, R. Vince, Conformationally restrained carbazolone-containing  $\alpha,\gamma$ -diketo acids as inhibitors of HIV integrase, *Bioorg. Med. Chem.* 14 (2006) 2942.
- [40] S.-I. Bascop, J.-Y. Laronze, J. Sapi, New dimethylaminoalkyl substituted auxin derivatives, *Monat. Fur. Chem.* 130 (1999) 1159–1166.